Production and decay of random kinetic energy in granular snow avalanches

Othmar BUSER, Perry BARTELT

WSL, Swiss Federal Institute for Snow and Avalanche Research SLF, Flüelastrasse 11, CH-7260 Davos-Dorf, Switzerland
E-mail: bartelt@slf.ch

ABSTRACT. Any model of snow avalanches must be able to reproduce velocity profiles. This is a key problem in avalanche science because the profiles are the result of a multitude of snow/ice particle interactions that, in the end, define the rheology of flowing snow. Recent measurements on real-scale avalanches show that the velocity profiles change from a highly sheared profile at the avalanche front to a plug-like profile at the avalanche tail, preventing the application of a single, simple rheology to the avalanche problem. In this paper, we model not only the velocity profiles but also the evolution of the velocity profiles, by taking into account the production and decay of the kinetic energy of the random motion of the snow granules. We find that the generation of this random energy depends on the distribution of viscous shearing within the avalanche. Conversely, the viscous shearing depends on the magnitude of the random energy and therefore its collisional dissipation. Thus, there is a self-consistency problem that must be resolved in order to predict the amount of random energy and therefore the velocity profiles. We solve this problem by stating equations that describe the production and decay of random energy in avalanches. An important guide to the form of these equations is that the generation of random energy is irreversible. We show that our approach successfully accounts for measured profiles in natural avalanches.

1. INTRODUCTION

A fundamental problem in avalanche science is to accurately describe the rheology of flowing snow. Solving this problem is central to developing avalanche-dynamics models that can reliably predict avalanche velocities and run-out distances in general, three-dimensional terrain. This problem is especially difficult since the rheology of flowing snow is governed by the shearing and collisional interactions of millions of hard snow/ice particles. Although, in principle, it would be possible to calculate the trajectory of every particle in such a many-bodied system, many practical difficulties would still remain, such as the problem of particle formation and their certain abrasive degradation; the problem of the granule size and shape distributions; and quantifying the collisional properties of the granules as a function of temperature and frequency of collisions. The number of particles, the massive number of interactions and the uncertainty of the initial and boundary conditions make a purely dynamical description of snow avalanches both unfeasible and impractical.

In this paper, we address the avalanche problem at the level of the macroscopic properties of the granular system, not at the level of the individual particle trajectories. Our goal is to find a reduced description of the flow rheology that accounts for the granular interactions without over-simplifying the problem by lumping the granular effects into a single constitutive parameter such as an 'effective' viscosity or 'turbulent' friction (Salm, 1993). At the same time we avoid a formulation requiring the micro-collisional properties of the granules (coefficient of restitution) or the particle size and shape distributions (Jenkins and Savage, 1983; Hutter and others, 1987; Jenkins and Askari, 1994; Louge, 2003).

We describe the motion of an avalanche in simple shear in a two-dimensional coordinate system, x–z, by the superposition of the horizontal and vertical random velocity of the granules, $u_r(z, t)$ and $w_r(z, t)$, respectively, on the

corresponding laminar (the velocity parallel to the slope), steady-on-average flow fields, $\overline{u}(z)$ and $\overline{w}(z)$ (Fig. 1):

$$u(z, t) = \overline{u}(z) + u_r(z, t) \quad \text{and} \quad w(z, t) = \overline{w}(z) + w_r(z, t), \quad (1)$$

where $\overline{u}(z)$ and $\overline{w}(z)$ are given by

$$\overline{u}(z) = \langle u(z, t) \rangle \quad \text{and} \quad \overline{w}(z) = 0. \quad (2)$$

Let f^2 be the mean-square random velocity

$$f^2(z, t) = u_r^2(z, t) + w_r^2(z, t). \quad (3)$$

Then the translational (in the direction of flow) and random kinetic energies of the avalanche are

$$K(z) = \rho \left(\frac{\overline{u}^2(z)}{2} \right) \quad \text{and} \quad R(z) = \rho \left(\frac{f^2(z)}{2} \right), \quad (4)$$

respectively, where ρ is the avalanche density. In this paper, granular effects are characterized by the distribution of random kinetic energy of the particles, $R(z)$. Note that the sum of $K(z)$ and $R(z)$ is the total kinetic energy of the particles.

The evolution in time of the function $R(z)$ is the sum of two different processes. The random velocity of the particles varies both as (1) a result of the viscous shear work done on the particle and (2) a result of the inelastic collisions between particles. These granular processes define two additional macroscopic energy fluxes. In this paper, we are confronted with the problem of calculating, *on average*, how the random kinetic energy is produced by the available shear work (the source of $R(z)$, the first energy flux) and how it decays by collisions (the sink of $R(z)$, the second energy flux). In conventional avalanche models, the energy fluxes are the reversible transformation of potential energy to translational kinetic energy, K, and the irreversible transformation of the mechanical energy to heat, internal energy, E.
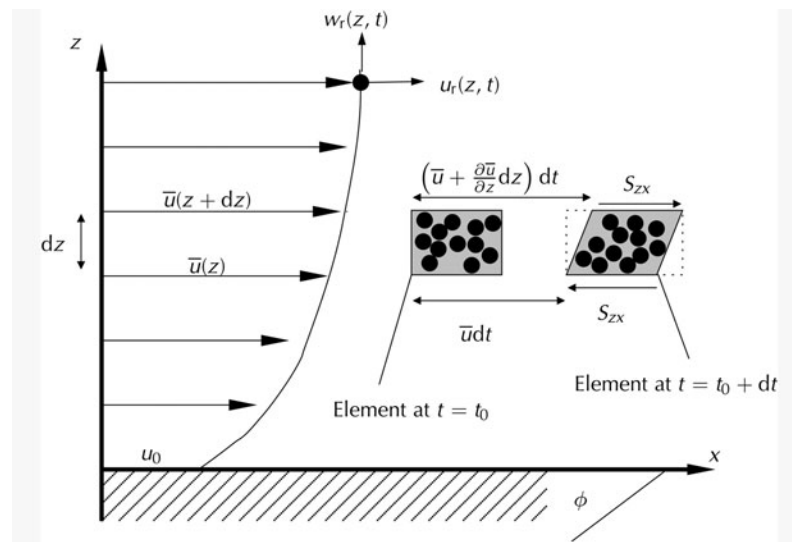
Fig. 1. Velocity distribution and shear stress for an avalanche in simple shear.

Although K and R are both kinetic energies, they possess a fundamental difference: the transformation of potential energy to translational kinetic energy is reversible, whereas the production of random kinetic energy is irreversible. The irreversibility of R can be shown by considering the mechanical work done by the random forces, W_r, arising from the random motion of the snow clods:

$$W_r = \int_x F_r(t)\, dx = 0, \tag{5}$$

where $F_r(t)$ is the *resultant* force of the random collisional processes per unit area in the direction of the flow, x (Bartelt and others, 2006). The mean value – over a large enough time interval – in the integral Equation (5) is zero since the random forces, $F_r(t)$, arise from random velocities,

$$\langle F_r(t)\rangle = 0. \tag{6}$$

Moreover, the force, $F_r(t)$, averaged over time must be zero, since it arises from the random motion which is without bias (Langevin, 1908). Since the random fluctuations can do no work in the mean over time, they cannot produce a change in the translational kinetic energy of the avalanche (by the work–energy theorem). This is similar to turbulence theory where the fictitious Reynolds stresses, arising from averaging of the velocity fluctuations, cannot create or destroy mechanical energy (Davidson, 2004). The fluctuating motion of the snow granules can only decay by collisional processes, producing heat and only heat. Therefore, we cannot place energy into the random motion of the granules and then extract the energy to increase the potential energy of the system. The irreversibility of the random energy implies that it is a type of internal energy, similar to heat, but not yet heat. However, unlike heat, R must disappear when the avalanche stops.

The primary goal of this paper is, therefore, to exploit the random-energy fluxes to develop new constitutive models for avalanche flow. Since the production of $R(z)$ is the result of internal shearing, which is defined by the constitutive model, the constitutive equations not only define how mechanical energy is dissipated, but also the *source* of the random energy. A constitutive model no longer describes a single process (viscous dissipation); now the model must additionally describe the interaction between the viscous and collisional processes. These two processes must be symmetric in the sense that the total dissipation remains constant: the amount the viscous process does not dissipate is left to the collisional process. We demonstrate this result by modifying an existing model for avalanche flow (Norem and others, 1987) and then predicting the *evolution* of measured velocity gradients in real-scale avalanches.

2. PRODUCTION AND DECAY OF RANDOM ENERGY

Conservation of energy demands that the sum of the rate of change of the total energy inside a volume element within the avalanche is equal to the rate of work done by the external forces (Anderson, 1996; Davidson, 2004):

$$\frac{d}{dt}(K + E) = \dot{K} + \dot{E} = \dot{W}_g - \dot{W}_f, \tag{7}$$

where $\dot{K}$ is the rate of change of translational kinetic energy per unit volume, $\dot{W}_g$ is the *positive* work rate of gravity and $\dot{W}_f$ is the *always negative* rate of frictional work done by viscous shear forces (or frictional work rate). The quantity $\dot{E}$ is the rate of change in internal energy, including both the rise in heat, $\dot{\Phi}$, and the net random kinetic-energy change, $\dot{R}$:

$$\dot{E} = \dot{\Phi} + \dot{R}. \tag{8}$$

Although $\dot{R}$ is part of the total kinetic energy, we transfer it to the internal energy, $\dot{E}$, making use of the fact that both $\dot{\Phi}$ and $\dot{R}$ are irreversible and therefore contribute to the internal energy rise. The work done by gravity is equivalent to the change in potential energy of the avalanche, $\dot{U}_g$,

$$\dot{W}_g = -\dot{U}_g. \tag{9}$$

The negative sign arises because the *loss* of potential energy does *positive* work on the avalanche. Therefore, conservation of energy (Equation (7)) requires that

$$\frac{d}{dt}(K + U_g + E + W_f) = 0, \tag{10}$$

or, after substitution of Equation (8),

$$\frac{d}{dt}\left(K + U_g + \Phi + R + W_f\right) = 0. \qquad (11)$$

The frictional work rate can be decomposed into two parts (Davidson, 2004):

$$\dot{W}_f = \dot{W}_{f \longrightarrow K} + \dot{W}_{f \longrightarrow E}, \qquad (12)$$

where $\dot{W}_{f \longrightarrow K}$ represents the rate of increase of mechanical energy, the sum of the reversible kinetic and potential energies. That is, time rate of change in mechanical energy is

$$\dot{K} + \dot{U}_g = -\dot{W}_{f \longrightarrow K}. \qquad (13)$$

The remaining part of the frictional work rate, $\dot{W}_{f \longrightarrow E}$, increases the internal energy, $\dot{E}$:

$$\dot{E} = -\dot{W}_{f \longrightarrow E}. \qquad (14)$$

Because $\dot{W}_{f \longrightarrow E}$ is always negative, the increase in internal energy is always positive, in accordance with the second law of thermodynamics (Glansdorf and Prigogine, 1974). In steady state, the change in kinetic energy $\dot{K} = 0$. Therefore, we have from Equation (13)

$$\dot{U}_g + \dot{W}_{f \longrightarrow K} = -\dot{W}_g + \dot{W}_{f \longrightarrow K} = 0. \qquad (15)$$

The loss in potential energy is equal to the (negative) work done by the frictional forces (Bartelt and others, 2005). However, in order to achieve this mechanical steady state ($\dot{K} = 0$, constant translational velocity), the rate of change of the internal energy must likewise be zero ($\dot{E} = 0$, constant temperature rise). Since the internal energy is the sum of the irreversible thermal and random kinetic energies, this fact indicates that a steady state can only be achieved when the rate of change of random kinetic energy in the avalanche is $\dot{R} = 0$ (the random energy is constant).

It has often been assumed that the rate of internal energy rise is equivalent to the rise in thermal energy *only* (e.g. Salm, 1993), i.e. $\dot{E} = \dot{\Phi}$. We now suppose the mechanical work of the frictional forces raises the total internal energy of the avalanche, raising the thermal energy *and* creating random kinetic energy, R, at the rate, $\dot{R}$:

$$\dot{E} = -\dot{W}_{f \longrightarrow E} = \dot{R} + \dot{\Phi}. \qquad (16)$$

Let us consider $\dot{R}$ in detail. The simplest and most plausible assumption we can make is that R decays to heat (or internal energy) in proportion to its amount. The net change, $\dot{R}$, is part of the total kinetic-energy change, or total dissipation. However, since it is difficult to measure the total kinetic-energy change directly and we know the total dissipation (because we have some constitutive relation which fits the measurements), we have chosen to produce R by taking some fraction of the total dissipation. Thus,

$$\dot{R} = \alpha\dot{E} - \beta R = -\alpha\dot{W}_{f \longrightarrow E} - \beta R, \qquad (17)$$

where $-\alpha\dot{W}_{f \longrightarrow E}$ is the part of the frictional work rate producing random energy and βR is the decay of random energy (or heat produced) caused by the inelastic collisions of the snow granules. The rise in thermal energy must be

$$\dot{\Phi} = (1 - \alpha)\dot{E} + \beta R = -(1 - \alpha)\dot{W}_{f \longrightarrow E} + \beta R. \qquad (18)$$

The parameters α and β determine the production and decay of random energy, respectively, and therefore the total amount of random energy at any given time or position within the avalanche, $\alpha \in [0, 1]$ and $\beta \geq 0$. By addition
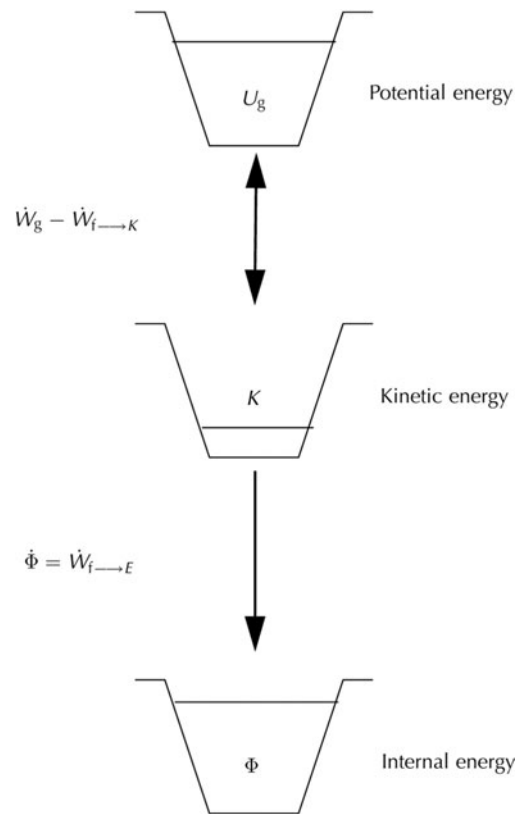

Fig. 2. Energy flow without random kinetic energy. Potential energy is converted into kinetic energy, K, and internal energy (heat), Φ. The reversibility of the kinetic energy is depicted with a double arrow.

of Equations (17) and (18), we recover Equation (16). This formulation satisfies energy conservation *always*, since we find by substitution of Equation (16) into Equation (10)

$$\frac{d}{dt}(R + \Phi + K) = \dot{W}_g - \dot{W}_f. \qquad (19)$$

The rate of change of the sum of the kinetic, thermal and random kinetic energies is equal to the rate of work done by gravity and frictional forces. Thus, this formulation, which now accounts for random kinetic energy, is *always* energy-conserving if the change in random energy, $\dot{R}$, is governed by a production–decay relation such as the one given by Equation (17).

3. ENERGY FLUXES IN AVALANCHES

The production and decay of random kinetic energy (Equation (17)) contains two additional energy fluxes. The traditional picture of energy transformations is that potential energy, U_g, the only energy source, is dissipated entirely to heat, Φ (Fig. 2). The increase or decrease of kinetic energy, K, depends on the sign of the sum of gravitational and frictional work rates. That is, if

$$
\begin{aligned}
\dot{W}_g - \dot{W}_{f \longrightarrow K} &> 0 \quad \text{(acceleration)} \\
\dot{W}_g - \dot{W}_{f \longrightarrow K} &= 0 \quad \text{(steady state)} \\
\dot{W}_g - \dot{W}_{f \longrightarrow K} &< 0 \quad \text{(deceleration)}.
\end{aligned}
\qquad (20)
$$

Since the energy exchange between U_g and K is reversible it is depicted in Figure 2 with a double arrow. Energy-balance calculations of natural avalanches captured at the Swiss Vallée de la Sionne test site indicate $0.1 < K/U_g < 0.2$.
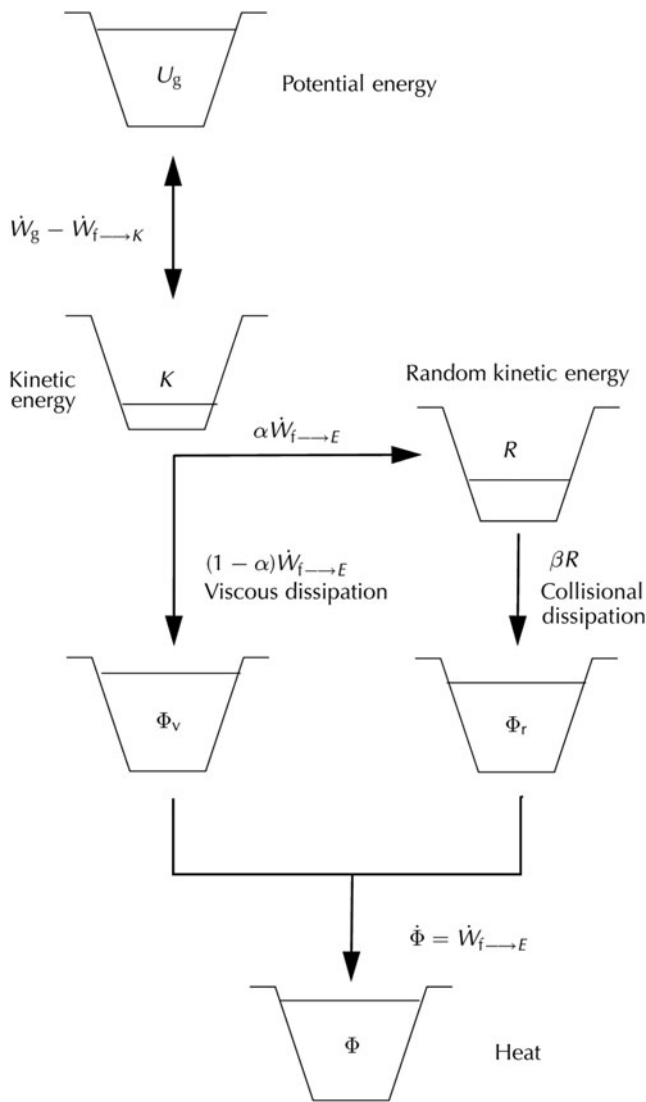
Fig. 3. Energy flow with random kinetic energy, R. The frictional work rate, $\dot{W}_{f\longrightarrow E}$, is divided into $\alpha\dot{W}_{f\longrightarrow E}$ (production of random kinetic energy) and $(1-\alpha)\dot{W}_{f\longrightarrow E}$. The random kinetic energy decays at the rate βR.

That is, only 10–20% of the available potential energy is transformed to kinetic energy (Sovilla and others, 2006).

Figure 3 depicts the modified energy flow in an avalanche, including the production and decay of random energy which is governed by Equation (17). The transfer of energy from the mean flow field to the random kinetic energy is governed by the production term, $\alpha\dot{W}_{f\longrightarrow E}$. As long as the avalanche is in motion, random kinetic energy can be generated. The remaining part of $(1-\alpha)\dot{W}_{f\longrightarrow E}$ is dissipated as heat. The random energy decays at the rate βR. The balance between the production term and the decay term determines whether the random energy intensifies, or begins to die away. When the avalanche stops, the generation of random energy ceases and the random energy disappears. When the production rate of random kinetic energy is equal to the collisional dissipation rate, there is no change in R ($\dot{R} = 0$). In this case, the avalanche might attain a steady flow state if the gravitational work rate (or driving force) is additionally in balance with $\dot{W}_{f\longrightarrow K}$ (or the frictional force). Since avalanches are finite mass flows, it is unlikely that such steady flow states can be maintained for long periods of time.

In fact, as the velocity of the avalanche decreases in the run-out zone, the decay of R will overcome the production. This process has been linked to avalanches starving on steep slopes (Bartelt and others, 2007).

4. AVALANCHE FLOW IN SIMPLE SHEAR

The energy arguments of the preceding section implicitly account for *gradients* of velocity produced by shearing tractions. To explicitly include the effect of shear gradients, we consider a fluid element in an avalanche of density ρ flowing down a slope of angle ϕ (Fig. 1). The forces acting on an element of the avalanche are divided into body forces (gravity) and surface tractions (shear stresses). For reasons of clarity, we restrict our analysis to a two-dimensional element in x–z space in simple shear. Therefore, shear stresses, S_{zx}, act on the upper and lower boundaries of the element, resisting motion in the x direction. The shearing tractions create a velocity distribution, $\overline{u}(z)$, in the z direction. The velocity gradient is $\partial\overline{u}(z)/\partial z$. The work done by gravity is

$$\dot{W}_g(z) = \rho g\left(\overline{u}(z)\sin(\phi)\right), \tag{21}$$

where g is gravitational acceleration. The frictional work rate is

$$\dot{W}_f(z) = \frac{\partial}{\partial z}(S_{zx}(z)\overline{u}(z)) = \overline{u}(z)\frac{\partial S_{zx}(z)}{\partial z} + S_{zx}(z)\frac{\partial\overline{u}(z)}{\partial z}. \tag{22}$$

The rate of change of the translational kinetic energy in the x direction (cf. Equation (13)) is

$$\dot{K}(z) = \rho g\left(\overline{u}(z)\sin(\phi)\right) + \overline{u}(z)\frac{\partial S_{zx}(z)}{\partial z}. \tag{23}$$

This equation is equivalent to the momentum equation in one dimension (Davidson, 2004). We find

$$\dot{W}_{f\longrightarrow K} = \overline{u}\frac{\partial S_{zx}}{\partial z} \tag{24}$$

and, subsequently, by Equation (12),

$$\dot{W}_{f\longrightarrow E} = S_{zx}\frac{\partial\overline{u}}{\partial z}. \tag{25}$$

Therefore, the production–decay equation for random kinetic energy for an avalanche in simple shear is

$$\frac{d}{dt}(R) = -\alpha\left(S_{zx}\frac{\partial\overline{u}}{\partial z}\right) - \beta R \tag{26}$$

and the corresponding change in thermal energy is given by

$$\frac{d}{dt}(\Phi) = -(1-\alpha)\left(S_{zx}\frac{\partial\overline{u}}{\partial z}\right) + \beta R. \tag{27}$$

Equations (26) and (27) can be modified to include energy transport by diffusion. Assuming Fourier-type laws for diffusion in both the x and z directions we find

$$\frac{D}{Dt}(R) = k_R\left(\frac{\partial^2 R}{\partial x^2} + \frac{\partial^2 R}{\partial z^2}\right) - \alpha\left(S_{zx}\frac{\partial\overline{u}}{\partial z}\right) - \beta R \tag{28}$$

and

$$\frac{D}{Dt}(\Phi) = k_T\left(\frac{\partial^2 T}{\partial x^2} + \frac{\partial^2 T}{\partial z^2}\right) - (1-\alpha)\left(S_{zx}\frac{\partial\overline{u}}{\partial z}\right) + \beta R, \tag{29}$$

where k_R and k_T are the conductivities of random and thermal energy. T is the true 'thermal' temperature of the avalanche (whereas R can be considered the 'granular' temperature). In the above equation we have, for completeness, replaced the time derivates of R and Φ with the substantial

derivatives. Therefore, the energy removed from the mean motion of the flow at one point need not represent the total heat or random kinetic energy at the same location. In this paper, we do not treat diffusion processes explicitly.

Since there are heat and random-energy fluxes through the bottom and top surface of the avalanche, Equations (28) and (29) must be supplemented with appropriate boundary conditions (Jenkins, 1992). Melt layers are often the result of the heat flux at the bottom of the avalanche. When random energy escapes a boundary, it is no longer random, since in the absence of collisions it will lose its non-directional quality. Beyond the upper surface, or avalanche front, random energy can be transformed to potential or kinetic energy.

5. CONSTITUTIVE MODEL

A constitutive equation for flowing snow must be able to model both solid- and fluid-flow behaviour. Several authors have therefore proposed writing the in-plane shear stress, $S_{zx}(z)$, (Fig. 1) as the sum of a Coulomb-like friction (accounting for the solid part with or without cohesion) and a viscous resistance (accounting for the fluid part). Norem and others (1987) generalized this idea and proposed an equation (in simple shear) of the form:

$$S_{zx}(z) = a + b\left(N(z)\right)^k + m\left(\dot{\gamma}(z)\right)^n, \qquad (30)$$

where a is the cohesion, b is the Coulomb friction coefficient operating on the normal or overburden stress, $N(z)$, and m is the shear viscosity. We, like Norem and others (1987), denote the shear rate

$$\dot{\gamma}(z) = \frac{\partial \overline{u}(z)}{\partial z}. \qquad (31)$$

Chute experiments with flowing snow (Platzer and others, 2007) show $k = 1$, indicating a linear relationship between normal stress, $N(z)$, and shear strength. Opinions differ on the choice of shear-rate exponent, n. Using experiments with granular materials as a guide, Norem and others (1987) proposed $n = 2$, following Bagnold (1954). Experiments with snow (Dent and Lang, 1983; Nishimura and Maeno, 1987) seem to suggest Newtonian behaviour ($n = 1$). To model 'plug' flows, which have been observed in many real-scale experiments (Dent and others, 1998; Kern and others, in press), the shear stresses must be higher than a (Dent and Lang, 1983; Nishimura and Maeno, 1987; Norem and others, 1987).

In the following we modify the constitutive equation (Equation (30)) to

$$S_{zx}(z) = bN(z) + \left(m - m'\right)\dot{\gamma}(z), \qquad (32)$$

where the parameter m' accounts for the shear thinning induced by collisional interactions within the fluidized region which requires $R(z) > 0$ (Salm and Gubler, 1985; Gubler, 1987). Moreover, $m' > 0$ when $R(z) > 0$ and $m' = 0$, when $R(z) = 0$. Thus, m represents the viscosity of the non-fluidized snow. This value is large, because it accounts for sintering processes between particles that can occur when the fluctuation energy is zero. We set $a = 0$, as we show it is possible to model plug flows in regions where $R(z) = 0$; that is, without assuming some material yield stress or cohesion. Clearly, $\left(m - m'\right) \geq 0$ always.

5.1. Symmetric interactions

The parameter m' can be found by noting that, at any given instant, the energy dissipated by viscous shearing is

$$\dot{\Phi}_v = (1 - \alpha)\left(m - m'\right)\dot{\gamma}(z)^2. \qquad (33)$$

The energy dissipated by the product of the overburden pressure and shear rate,

$$\dot{\Phi}_n = (1 - \alpha)bN(z)\dot{\gamma}(z), \qquad (34)$$

likewise contributes to the production of random kinetic energy (it is multiplied by $(1 - \alpha)$). The random energy transformed to heat energy is

$$\dot{\Phi}_r = \beta R. \qquad (35)$$

The reduction of viscous shearing by m' is entirely due to the amount of R. Assuming, additionally, that the main production of R is due to viscous shearing alone, we arrive at a self-consistent description of the interaction between viscous dissipation and random-energy production. This assumption does not influence the choice of a single parameter, β, to describe the decay of random energy. The decay of random energy must be independent of its origin. However, we should find that b is a constant.

By completing the square of the sum of the dissipated viscous ($\dot{\Phi}_v$) and random kinetic ($\dot{\Phi}_r$) energies, we therefore ensure that the division between these two dissipative processes always conserves the sum and the interaction is self-consistent. As stated in the introduction, any decrease in dissipation caused by the generation of random kinetic energy will eventually be balanced by a corresponding increase in collisional dissipation. This procedure ensures that the total irreversible energy is conserved and enforces that the random kinetic energy has a true one-way character: once it is created, it can only be transformed into heat. We therefore obtain a coefficient, m', of the form

$$m' = 2\frac{\psi}{(1 - \alpha)}\frac{\sqrt{R}}{\dot{\gamma}}, \qquad (36)$$

where

$$\psi = \sqrt{(1 - \alpha)m\beta}. \qquad (37)$$

This result, apart from its practical value (we have reduced the number of model parameters), shows an interesting property: it is symmetric within the two dissipating processes. To demonstrate this symmetry of the viscous and collisional processes, we let the symbols X_v and X_r denote the viscous shear and collisional processes which are defined in terms of the shear rate and the square root of the random kinetic energy:

$$\{X\} = \left\{ \begin{array}{c} X_v \\ X_r \end{array} \right\} = \left\{ \begin{array}{c} \dot{\gamma} \\ \sqrt{R} \end{array} \right\}. \qquad (38)$$

The sum of the viscous and collisional dissipation can be written as a quadratic equation in terms of X_v and X_r. The associated matrix form is

$$\dot{\Phi} = \{X\}^T [L] \{X\}, \qquad (39)$$

where $[L]$ is the matrix of the quadratic form:

$$[L] = \left[\begin{array}{cc} L_{vv} & L_{vr} \\ L_{rv} & L_{rr} \end{array} \right] = \left[\begin{array}{cc} (1 - \alpha)m & -\psi \\ -\psi & \beta \end{array} \right]. \qquad (40)$$
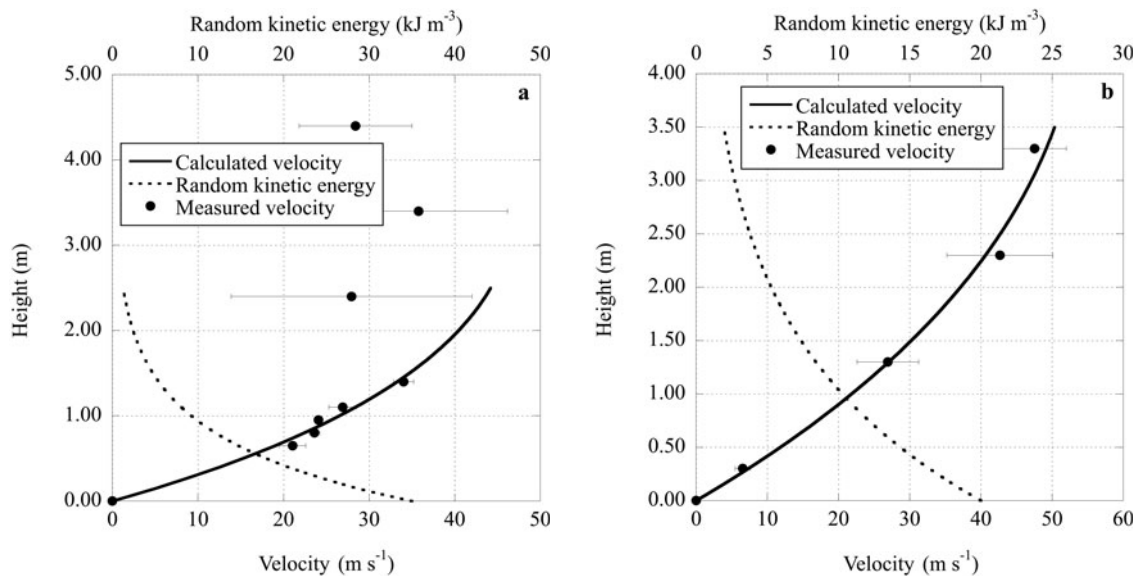
Fig. 4. Velocity profiles measured at the front of two avalanches and comparison to theory. (a) Avalanche No. 7226 (time interval [10 s, 12 s]) and (b) avalanche No. 816 (time interval [2.1 s, 5.4 s]). Constitutive parameters are listed in Table 1.

The constitutive formulation is such that $L_{rv} = L_{vr}$. Defining

$$\dot{\Phi}_{rv} = L_{rv} X_r X_v \qquad (41)$$

and

$$\dot{\Phi}_{vr} = L_{vr} X_v X_r \qquad (42)$$

we see that $L_{rv} = L_{vr} = -\psi$. The interaction between the viscous and collisional processes is constructed such that they are independent of the order of the product between X_v and X_r. This ensures that the interaction behind the viscous and collisional processes defines a unique, dissipative process. Of significance is the minus sign $(-\psi)$, for it implies that the *increase* of random kinetic energy produced by the viscous shearing and the *decrease* in heat production required to produce the random kinetic energy by viscous shearing *are equal*. We can write the dissipation as

$$\dot{\Phi}_v = J_v X_v \qquad (43)$$

$$\dot{\Phi}_r = J_r X_r, \qquad (44)$$

where J_v and J_r are:

$$J_v = (1 - \alpha) m X_v - \psi X_r \qquad (45)$$

$$J_r = -\psi X_v + \beta X_r. \qquad (46)$$

The diagonal components of the matrix $[L]$ are constant and satisfy the condition that

$$L_{ij} = \frac{\partial J_i}{\partial X_j} = \text{constant.} \qquad (47)$$

Therefore, the constitutive formulation is linear in X_v and X_r.

5.2. Vallée de la Sionne measurements

Kern and others (in press) obtained velocity profiles of three natural avalanches at different locations within flow using optical sensors (Tiefenbacher and Kern, 2004) located on the 20 m high mast at Vallée de la Sionne, canton Valais, Switzerland. For a detailed description of the site, see Sovilla and others (2006, 2008). These measurement results are used to formulate a constitutive model based on the production and decay of random kinetic energy. We begin with a brief description of the measured avalanches:

1. *Avalanche No. 7226, 21 January 2005.* On 21 January 2005 at 1500 h an avalanche naturally released. The measurement system was automatically triggered by geophones, and the recorded data indicate a dry, dense flowing avalanche. Moderate snowfall over several days had added ∼15 cm of new snow to the 105 cm thick snow cover in the release zone. Kern and others (in press) obtained three velocity profiles measured relative to the passage of the avalanche front ($t = 0$). These were located at time intervals [10 s, 12 s], [44.8 s, 44.9 s] and [55 s, 57 s]. The measured mean velocity behind the avalanche front was $U_m = 26.7 \, \text{m s}^{-1}$, but decreased rapidly towards the avalanche tail. The measured flow heights of the dense flowing part remained more-or-less constant for the three time intervals: $h \approx 2.4 \, \text{m}$. The velocity profiles change from a highly sheared profile at the front to a plug-like flow at the avalanche tail (Figs 4–6).

2. *Avalanche No. 816, 6 March 2006.* Between 2 and 4 March 2006, 120 cm of new snow was deposited in Vallée de la Sionne. On 5 March, the temperature rapidly dropped from −4 to −16°C in the release zone. The weather cleared and an avalanche was released artificially by explosives on the morning of 6 March. The released avalanche was dry-flowing with powder part. From the optical-sensor measurements, three velocity profiles could be ascertained in the flowing core at time intervals [2.1 s, 5.4 s], [32.4 s, 33.15 s] and [40.4 s, 42.5 s]. The measured mean velocity directly behind the avalanche front was $U_m = 32.2 \, \text{m s}^{-1}$. Similar to avalanche 7226, the velocity decreased rapidly towards the avalanche tail. Unlike avalanche 7226, the flow heights decreased from front to tail from $h \approx 3.5 \, \text{m}$ to $h \approx 1.6 \, \text{m}$. Again, the velocity profiles evolved from a highly sheared profile at the front to a plug-like flow at the avalanche tail (Figs 4–6).

3. *Avalanche No. 8448, 1 March 2007.* A heavy snowfall started at midday on 1 March 2007, accumulating ∼60–70 cm of new snow on the existing, 2.6 m thick, snow cover in the release area. The snowfall lasted until the early morning of 2 March. During the snowfall,
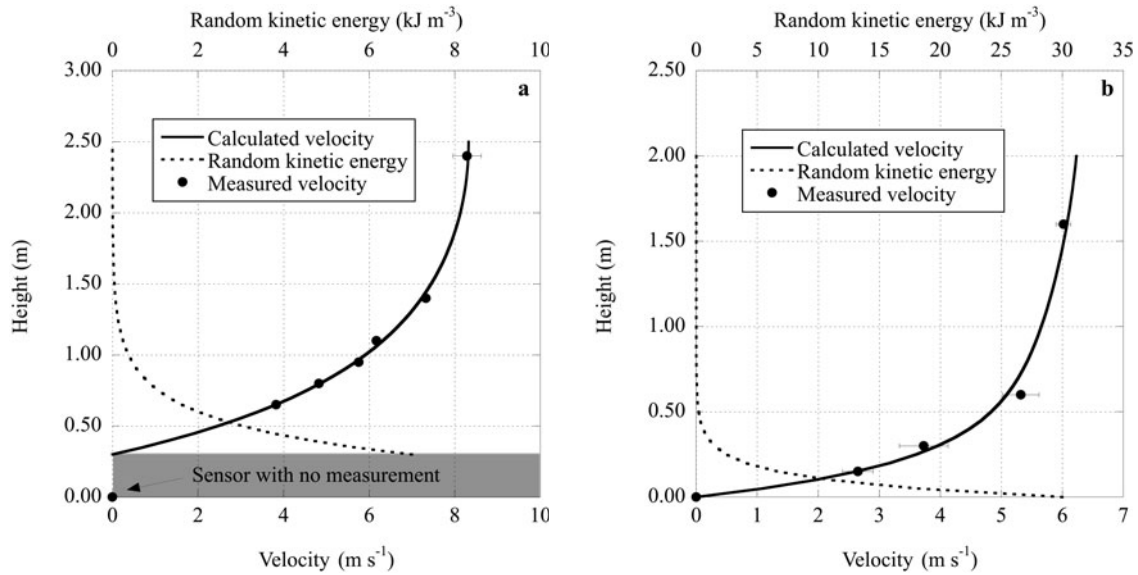
Fig. 5. Velocity profiles measured in the bulk of two avalanches and comparison to theory. (a) Avalanche No. 7226 (time interval [44.8 s, 44.9 s]) and (b) avalanche No. 816 (time interval [32.4 s, 33.15 s]). Constitutive parameters are listed in Table 1.
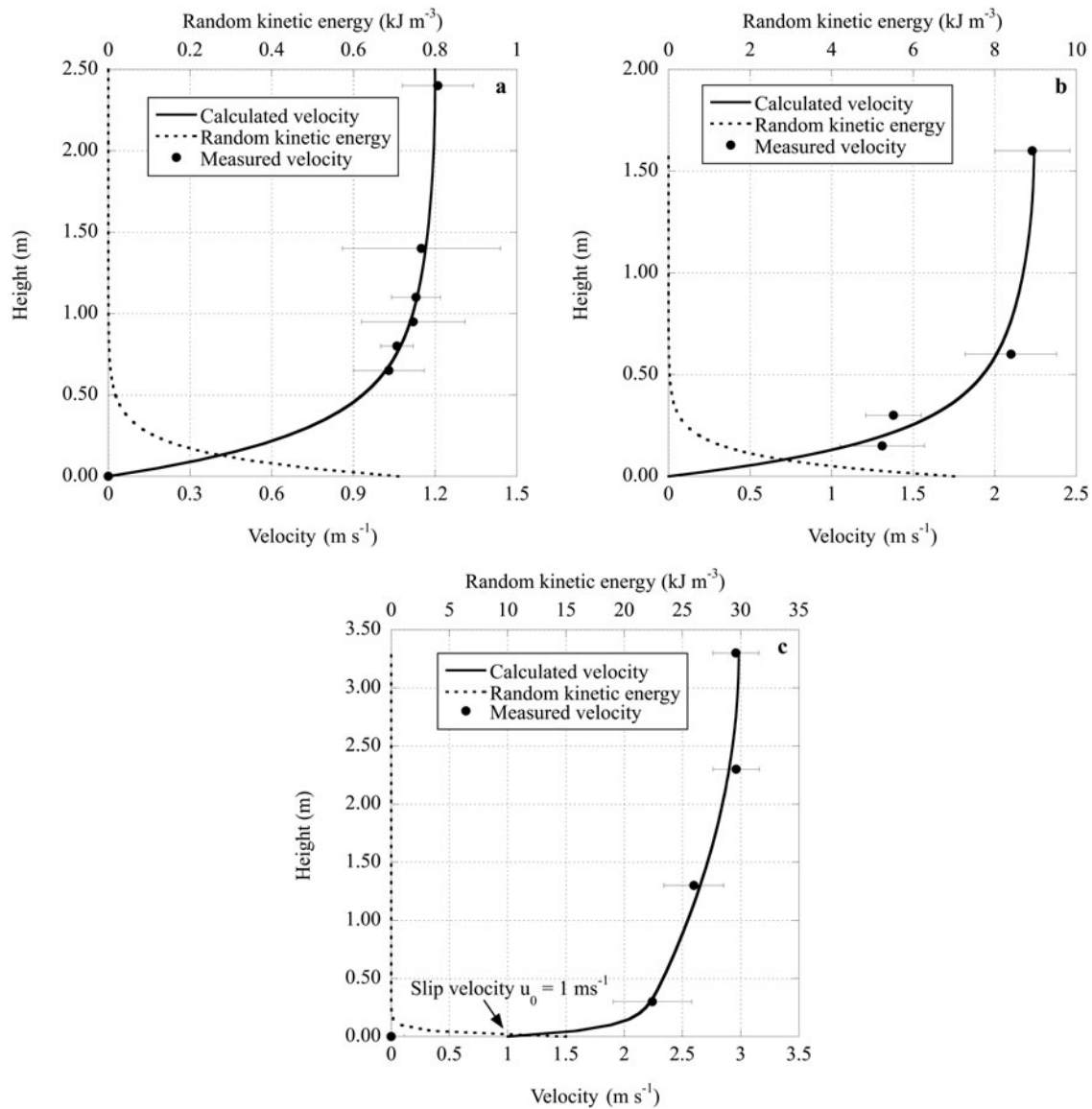

Fig. 6. Velocity profiles measured at the tail of three avalanches and comparison to theory. (a) Avalanche No. 7226 (time interval [55 s, 57 s]), (b) avalanche No. 816 (time interval [40.4 s, 42.5 s]) and (c) avalanche No. 8448 (time interval [72 s, 74 s]). Constitutive parameters are listed in Table 1.

Table 1. Mean velocity, flow height, penetration depth, mean random kinetic energy and values of constitutive parameters for three Vallée de la Sionne avalanches at the measured time interval

Avalanche	Time behind front	Mean velocity, U_m	Flow height, h	Penetration depth, z_0	Random energy, R_m	Coulomb friction, b	Production/decay, $\beta/(1-\alpha)$	Goodness of fit
	s	$m\,s^{-1}$	m	m	$kJ\,m^{-3}$		s^{-1}	
7226	[10, 12]	29.6	2.75	0.750	9.30	0.1252 ± 0.0169	0.9870 ± 0.0321	0.9928
7226	[44.8, 44.9]	5.4	2.40	0.240	0.70	0.2554 ± 0.0093	1.0737 ± 0.0508	0.9995
7226	[55, 57]	1.0	2.40	0.135	0.04	0.3214 ± 0.0007	1.0336 ± 0.0242	0.9996
816	[2.1, 5.4]	30.9	3.50	1.500	7.74	0.1607 ± 0.0109	0.7708 ± 0.0216	0.9979
816	[32.4, 33.15]	5.4	2.50	0.100	1.20	0.2916 ± 0.0087	0.8818 ± 0.0511	0.9976
816	[40.4, 42.5]	1.9	1.60	0.090	0.39	0.3046 ± 0.0207	0.7271 ± 0.1251	0.9828
8448	[72, 74]	2.6	3.30	0.034	0.15	0.3148 ± 0.0009	0.8424 ± 0.0464	0.9986

there was moderate wind from westerly directions with speeds up to $10\,m\,s^{-1}$. The temperature was about $-4°C$ in the release zone and slightly above $0°C$ in the run-out. After an accumulation of $\sim 40\,cm$ of new snow, an avalanche released spontaneously at 2119 h. The avalanche exhibited typical wet, dense, slow flow. Only one velocity profile could be obtained from the velocity sensors. This was at the tail of the flow at time interval [72 s, 74 s]. The mean speed of the avalanche at this stage was small, only $U_m = 2.6\,m\,s^{-1}$; however, the flow height was large, $h \approx 3.3\,m$.

5.3. Comparison to measured velocity profiles

The velocity profiles, $u(z)$, are found by solving the momentum-balance equation (Anderson, 1996)

$$\frac{\partial S_{zx}}{\partial z} + G_x = 0, \quad u(0) = u_0 \quad \text{and} \quad S_{zx}(h) = 0, \quad (48)$$

where G_x is the gravitational-body force $G_x = \rho gh\sin(\phi)$. The model requires four constitutive parameters (α, β, b and m) to fit the measurements. For all the measurements, we assumed a constant non-fluidized snow viscosity of $m = 200\,Pa\,s$, based on snow-chute experiments (Kern and others, 2004), and a constant flow density $\rho = 350\,kg\,m^{-3}$. The value of fluidization viscosity, m', is a function of a combination of α and β, as well as the random kinetic energy distribution, $R(z)$ (Equation (36)). Because we measure the velocity profiles at only one position in the avalanche (as it passes the mast) we cannot separate the production and decay coefficients and therefore combine α and β into a single parameter, $\beta/(1-\alpha)$. We apply a least-squares fitting procedure to find parameters b and $\beta/(1-\alpha)$. Following earlier work (Salm and Gubler, 1985; Gubler, 1987), we assume that the distribution of random kinetic energy is largest at the running surface where the product of the shear stress and velocity gradient is the largest

$$R(z) = R_0 \exp\left(-z/z_0\right), \quad (49)$$

where R_0 is the random kinetic energy at $z = 0$ and z_0 defines the penetration depth of the energy from the basal surface. This assumption is based on measurements of internal avalanche velocities with radar (Gubler and others, 1986). Bartelt and others (2006) also found an exponential decrease in random kinetic energy in the upper regions of the avalanche flow, when the production of random energy is concentrated in a 'slip volume', located near the basal

surface. With this procedure, they were able to fit velocity profiles of snow-chute experiments.

Comparisons between the large-scale avalanche measurements at Vallée de la Sionne and the solution to Equation (48) are depicted in Figures 4 (behind the avalanche front), 5 (interior) and 6 (avalanche tails). The fit parameters, including the goodness of fit and the fit errors, are reported in Table 1. The reported values of b for the avalanche tails are in good agreement with values reported by Lang and Dent (1983) and Platzer and others (2007). Only at the tail of avalanche 8448 did we assume a slip velocity, $u_0 = 1\,m\,s^{-1}$; otherwise $u_0 = 0$. The mean velocity given in Table 1 is

$$U_m = \frac{1}{h}\int_0^h u(z)\,dz. \quad (50)$$

Values of the penetration depth are also provided in Table 1. The mean random kinetic energy, R_m, is calculated according to

$$R_m = \frac{1}{h}\int_0^h R(z)\,dz. \quad (51)$$

The mean random kinetic energy decays exponentially as a function of the position behind the avalanche front (which we measure as the time behind the leading edge of the avalanche; Fig. 7). The results of our comparison suggest that the random energy is created largely at the avalanche front, but, as the dense core of the avalanche follows, is rapidly destroyed. The random energy decreases from front to tail. The coefficient of friction, b, is smaller at higher R_m (Fig. 8).

6. CONCLUSIONS AND OUTLOOK

By introducing the random kinetic energy, R, into an existing constitutive model we are able to predict the velocity profiles for different avalanches, as well as the evolution of the profiles from the avalanche front to tail. In the proposed model, each parameter has a physical meaning: the parameter m describes viscous shear resistance, $R = 0$; α is the degree of particle scattering induced by shear traction and β is the decay of the random kinetic energy by inelastic collisions. The scattering parameter, α, appears to depend on the inhomogeneities of the shearing plane and especially on the roughness of the boundary. The inverse quantity, $1/\beta$, can be considered to be the lifetime of the fluctuation energy and is a function of the collisional properties of the snow, such as the restitution coefficient. The comparison to the measured velocity profiles indicates a decrease in random
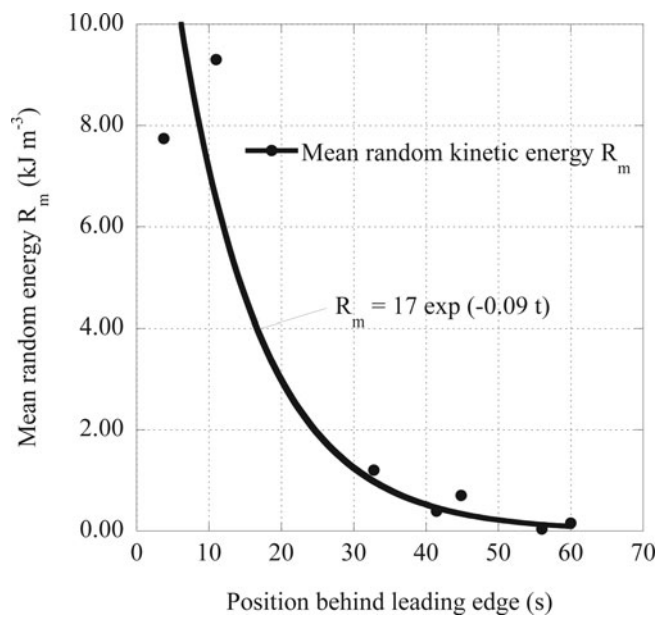
Fig. 7. Mean random kinetic energy calculated from velocity profiles as a function of time behind the leading edge of the avalanche. The random kinetic energy decays exponentially from front to tail. All avalanches.
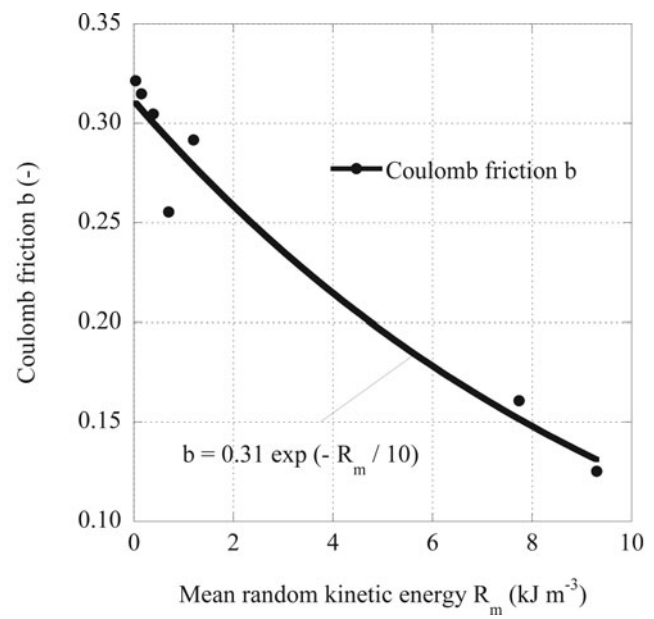

Fig. 8. Measurements from Vallée de la Sionne, revealing that the ratio of b changes exponentially with the mean random kinetic energy, R_m. All avalanches.

kinetic energy from front to tail of the avalanche. Therefore $1/\beta$ is much smaller than 50 s, the approximate time it takes for the avalanche to pass the measurement location.

The parameter b describes the influence of the overburden pressure on the shear resistance. In our comparison with the measured velocity profiles we found b could be written as an exponential function of R. Therefore,

$$\frac{\mathrm{d}b}{\mathrm{d}R} = -\frac{b}{R_b} \qquad \text{with} \qquad b(R=0) = b_0, \qquad (52)$$

where $R_b = 10 \, \mathrm{kJ} \, \mathrm{m}^{-3}$ and $b_0 = 0.32$. Moreover, the exponential relationship reflects the fact that the change in b with respect to R is a function of b itself. Thus, Equation (52) indicates that shear resistance depends on the magnitude of the random energy while, conversely, the magnitude of the random energy depends on the shear. This result suggests a more complex interaction between Coulomb friction and the production of random kinetic energy than we assumed in the constitutive equation (32). Interestingly, the lowest b values we encountered are in good agreement with values found for extreme avalanche calculations with numerical models (Gruber and Bartelt, 2007).

Also note that the penetration depth of random energy decays exponentially from front to tail (Fig. 9). At the avalanche front, the penetration depth reaches half the measured avalanche flow height: $z_0/h \approx 0.5$. The model predicts that random energy, and therefore mass, escapes the top surface of the avalanche (Fig. 4). Interestingly, a powder cloud developed at the front of both avalanches 7226 and 816. Towards the avalanche tail the penetration depth decays to values $z_0/h < 0.1$, resulting in plug-like flows. The random energy does not reach the top surface.

The energy approach does not rely on stationary flow states. Because we are concerned with energy fluxes, more insight is gained from the experiments when the fluxes are not in balance (i.e. when the avalanche is outside of steady-state equilibrium) and the production and decay of random energy can be differentiated and therefore separately

quantified. In steady state, it is impossible to distinguish between the production and decay of random energy and viscous dissipation. In this case, the rheology of a granular avalanche can be well described by an effective viscosity, or by adjusting the free parameters of the corresponding constitutive law. Fortunately, avalanches are hardly in steady state for long time intervals. In future this should allow us to identify the time-dependent production, diffusion and decay of random kinetic energy.

The penetration depth, z_0, is determined by the diffusion and lifetime of the random energy. We could not separate diffusion and penetration depth because the spatial transport of random kinetic energy is inherently a time-dependent process, which reveals itself only indirectly in the measured
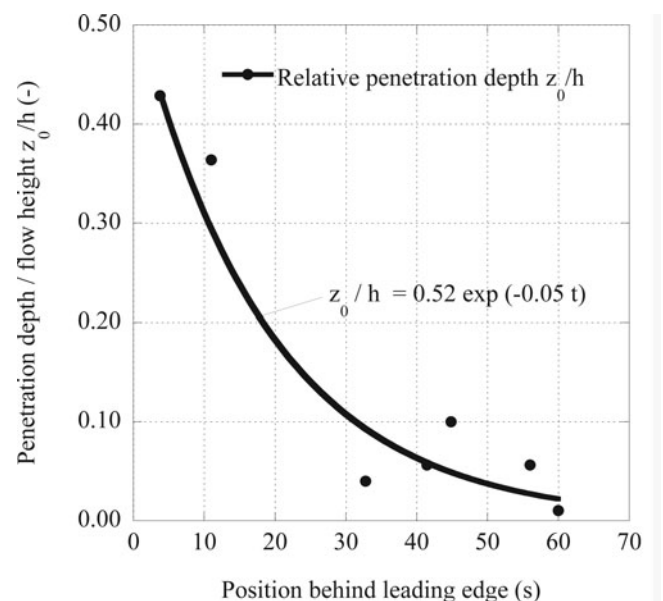

Fig. 9. Measurements from Vallée de la Sionne show that the ratio of z_0/h decays exponentially in time. All avalanches.

velocity profiles. Interestingly, we found that at the front of two avalanches the random kinetic energy reached the top surface of the flow. When this occurs, the random energy is confronted with a density change. At this point the directionlessness and randomness of the kinetic energy is lost. Mass must escape the top surface of the avalanche. Future investigations will show if the diffusion of random kinetic energy describes the initiation of a powder-snow avalanche.

Our constitutive proposal, combining the viscous and collisional dissipative processes, is a quadratic function in the shear rate, $\dot\gamma$, and the square root of the random kinetic energy, $\sqrt{R}$. Amazingly, it is both linear and symmetric. According to Glansdorf and Prigogine (1974), this would imply minimum entropy production if the avalanche was in steady state.

REFERENCES

Anderson, J.D. Jr. 1996. *Computational fluid dynamics: the basics with applications.* New York, McGraw-Hill.

Bagnold, R.A. 1954. Experiments on a gravity-free dispersion of large solid spheres in a Newtonian fluid under shear. *Proc. R. Soc. London, Ser. A,* **225**(1160), 49–63.

Bartelt, P., O. Buser and M. Kern. 2005. Dissipated work, stability and the internal flow structure of granular snow avalanches. *J. Glaciol.,* **51**(172), 125–138.

Bartelt, P., O. Buser and K. Platzer. 2006. Fluctuation–dissipation relations for granular snow avalanches. *J. Glaciol.,* **52**(179), 631–643.

Bartelt, P., O. Buser and K. Platzer. 2007. Starving avalanches: frictional mechanisms at the tails of finite-sized mass movements. *Geophys. Res. Lett.,* **34**(20), L20407. (10.1029/2007GL031352.)

Davidson, P.A. 2004. *Turbulence: an introduction for scientists and engineers.* Oxford, etc., Oxford University Press.

Dent, J.D. and T.E. Lang. 1983. A biviscous modified Bingham model of snow avalanche motion. *Ann. Glaciol.,* **4**, 42–46.

Dent, J.D., K.J. Burrell, D.S. Schmidt, M.Y. Louge, E.E. Adams and T.G. Jazbutis. 1998. Density, velocity and friction measurements in a dry-snow avalanche. *Ann. Glaciol.,* **26**, 247–252.

Glansdorf, P. and I. Prigogine. 1974. *Thermodynamic theory of structure, stability and fluctuations.* London, Wiley-Interscience.

Gruber, U. and P. Bartelt. 2007. Snow avalanche hazard modelling of large areas using shallow water numerical methods and GIS. *Environ. Model. Softw.,* **22**(10), 1472–1481.

Gubler, H. 1987. Measurements and modelling of snow avalanche speeds. *IAHS Publ.* 162 (Symposium at Davos 1986 – *Avalanche Formation, Movement and Effects*), 405–420.

Gubler, H., M. Hiller, G. Klausegger and U. Suter. 1986. Messungen an Fliesslawinen. Zwischenbericht 1986. *Eidg. Inst. Schnee- und Lawinenforsch. Mitt.* 41.

Hutter, K., F. Szidarovszky and S. Yakowitz. 1987. Granular shear flows as models for flow avalanches. *IAHS Publ.* 162 (Symposium at Davos 1986 – *Avalanche Formation, Movement and Effects*), 381–394.

Jenkins, J.T. 1992. Boundary conditions for rapid granular flow: flat, frictional walls. *J. Appl. Mech.,* **59**(1), 120–127.

Jenkins, J.T. and E. Askari. 1994. Hydraulic theory of a debris flow supported by a collisional shear layer. *In* Armanini, A., ed. *Proceedings of the International Workshop on Floods and Inundations Related to Large Earth Movements, 4–7 October 1994, Trento, Italy.* Delft, International Association of Hydraulic Research, A6.1–A6.10.

Jenkins, J.T. and S.B. Savage. 1983. A theory for the rapid flow of identical, smooth, nearly elastic spherical particles. *J. Fluid Mech.,* **130**, 187–202.

Kern, M., F. Tiefenbacher and J. McElwaine. 2004. The rheology of snow in large chute flows. *Cold Reg. Sci. Technol.,* **39**(2–3), 181–192.

Kern, M., P. Bartelt, B. Sovilla and O. Buser. In press. Measured shear rates in large dry and wet snow avalanches. *J. Glaciol.*

Lang, T.E. and J.D. Dent. 1983. Basal surface-layer properties in flowing snow. *Ann. Glaciol.,* **4**, 158–162.

Langevin, P. 1908. Sur la théorie du mouvement brownien. *C.R. Acad. Sci. [Paris],* **146**, 530–533.

Louge, M.Y. 2003. Model for dense granular flows down bumpy inclines. *Phys. Rev. E,* **67**(6), 061303. (10.1103/PhysRevE.67.061303.)

Nishimura, K. and N. Maeno. 1987. Experiments on snow-avalanche dynamics. *IAHS Publ.* 162 (Symposium at Davos 1986 – *Avalanche Formation, Movement and Effects*), 395–404.

Norem, H., F. Irgens and B. Schieldrop. 1987. A continuum model for calculating snow avalanche velocities. *IAHS Publ.* 162 (Symposium at Davos 1986 – *Avalanche Formation, Movement and Effects*), 363–379.

Platzer, K., P. Bartelt and M. Kern. 2007. Measurements of dense snow avalanche basal shear to normal stress ratios (S/N). *Geophys. Res. Lett.,* **34**(7), L07501. (10.1029/2006GL028670.)

Salm, B. 1993. Flow, flow transition and runout distances of flowing avalanches. *Ann. Glaciol.,* **18**, 221–226.

Salm, B. and H. Gubler. 1985. Measurement and analysis of the motion of dense flow avalanches. *Ann. Glaciol.,* **6**, 26–34.

Sovilla, B., P. Burlando and P. Bartelt. 2006. Field experiments and numerical modelling of mass entrainment in snow avalanches. *J. Geophys. Res.,* **111**(F3), F03007. (10.1029/2005JF000391.)

Sovilla, B., M. Schaer, M. Kern and P. Bartelt. 2008. Impact pressures and flow regimes in dense snow avalanches observed at the Vallée de la Sionne test site. *J. Geophys. Res.,* **113**(F1), F01010. (10.1029/2006JF000688.)

Tiefenbacher, F. and M. Kern. 2004. Experimental devices to determine snow avalanche basal friction and velocity profiles. *Cold Reg. Sci. Technol.,* **38**(1), 17–30.

MS received 5 August 2008 and accepted in revised form 28 December 2008